ICASSP 2023 - 2023 IEEE International Conference on Acoustics, Speech and Signal Processing (ICASSP) | 978-1-7281-6327-7/23/$31.00 ©2023 IEEE | DOI: 10.1109/ICASSP49357.2023.10094594

FLEXIBLE BEAM DESIGN FOR VITAL SIGN MONITORING USING A PHASED ARRAY EQUIPPED WITH DOUBLE-PHASE SHIFTERS

Zhaoyi Xu, Donglin Gao, Shuping Li, Chung-Tse Michael Wu and Athina Petropulu

Dept. of Electrical and Computer Engineering, Rutgers University

ABSTRACT

Recognizing the low-cost advantage of phased arrays, we investigate the improvement of the beamforming capability of a phased array via the use of double-phase shifters (DPS), i.e., each antenna is fed with the sum of the outputs of two phase shifters. The use of DPS allows for the manipulation of both the magnitude and phase of the signal transmitted by each antenna, thus enabling the formation of a flexible beam toward the desired target while suppressing the energy radiated toward unwanted directions. By sequentially steering the mainbeam to each target, while nulling other targets, one can monitor the vital signals of multiple targets with low inter-target interference. This is achieved at only a modest increase in the cost of a phased array due to the addition of phase shifters. The performance of the proposed approach is demonstrated via a prototype DPS phased array with 4 Vivaldi antennas using 8 commercial phase shifters and transmitting a continuous-wave RF signal at center frequency of 2.2 GHz.

***Index Terms*—** Vital sign monitoring, Phased array, Double-phase shifters.

1. INTRODUCTION

Vital signs, including breathing rate (BR) and heartbeat rate (HR), provide crucial insights into the physiological state of an individual. Traditional vital sign monitoring usually requires hospitalization and involves sensors that are attached to the body, such as photoplethysmography (PPG) and electrocardiogram (ECG) sensors. To overcome these problems, research studies have been exploring contactless vital sign monitoring via radar devices [1–7]. Phased arrays, the most widely used, low-cost radar have been the preferred monitoring devices [5, 6, 8].

In a conventional phased array, all the antenna elements are connected to a single radio-frequency (RF) chain through phase shifters, which are controlled by a computer. The phases are determined so that the transmitted signals add up coherently in the desired direction. By changing the phases, the formulated beam can be steered to different directions. However, in multi-target vital sign monitoring scenarios, there are no degrees of freedom for a conventional phased array to design a beam that can focus the energy on one target while at the same time reducing the energy radiated towards other directions. Thus, a phased array may excite multiple targets of no interest, which will then create interference during the estimation of the parameters of the target of interest. Of course, one could leverage an active electronically scanned array (AESA) for monitoring, where each antenna element is connected to the RF chain through a transmit/receive (T/R) module which enables controllable magnitude and phase [9]. However, while the AESA radar can synthesize a more complex beampattern, the multiple T/R modules increase the cost of the array [9]. One could also use a MIMO radar, which allows for flexible beam design [7]. However, MIMO radar require multiple RF chains which would significantly increase the hardware cost.

In our previous work [10], we proposed a low-cost way to improve the beamforming capability of a phased array by endowing it with more degrees of freedom via the use of double-phase shifters (DPS). Each antenna is connected to the sole RF chain via two phase shifters. In that configuration, one can control both the magnitude and the phase of the waveform transmitted by each antenna, thus enabling a more complex beampattern design capability. In this paper, we design and build a DPS phased array, and test its performance in multi-target vital sign monitoring. In particular, we designed and fabricated a four-antenna DPS phased array transmitter prototype, comprising a commercial power divider, 8 voltage-controlled phase shifters and two sets of one-to-four-to-two Wilkinson power divider network. By modifying the phase as well the magnitude of each antenna, a complex beampattern can be formulated to focus the energy towards the desired target while nulling the undesired targets. Although we had intended to run experiments with humans, the device needed a new institutional review board (IRB) protocol approval, which was not ready at the time of submission of this paper. Therefore, instead of human targets, we conducted experiments using actuators with metal boards to approximate the human chest.

2. PHASED ARRAY WITH DOUBLE-PHASE SHIFTERS

Let us consider a phased array, consisting of a single RF chain, feeding a uniform linear array (ULA) of N transmit antennas (TX), spaced by d (see left part of Fig. 1). The

Work supported by NSF under grant ECCS-2033433.

antennas transmit a weighted narrow-band signal with wavelength λ. The array output at time t towards angle θ is

$$y(t,\theta) = \mathbf{a}^H(\theta)\mathbf{w}x(t), \tag{1}$$

where $\mathbf{a}(\theta) = [1, e^{j2\pi d\frac{\sin\theta}{\lambda}}, \ldots, e^{j2\pi(N-1)d\frac{\sin\theta}{\lambda}}]^T$ is the steering vector at direction θ; $\mathbf{w} \in \mathbb{C}^{N\times 1}$ is the weight vector, whose elements have unit modulus; and $x(t)$ is the unit energy baseband signal at time t.

On setting $\mathbf{w} = \mathbf{a}(\theta_0)$, where θ_0 is the beamforming angle, the signals transmitted by the antennas will add up coherently at θ_0 as $y(t,\theta_0) = \mathbf{a}^H(\theta_0)\mathbf{a}(\theta_0)x(t) = Nx(t)$. The conventional phased array relies on computer-controlled unit-modulus weights. Thus, it can only formulate a beam focusing the power in one direction, while it has no control over the power radiated in other directions. In multi-target vital sign monitoring, especially when the targets are closely spaced, the phased array may excite targets falling in the sidelobes of the beam, which will then interfere the monitoring of the target of interest.

To improve the beamforming capability of a phased array we investigate the use of double-phase shifters (DPS) [10]. In particular, each antenna is connected to the sole RF chain via two phase shifters as shown on the right side of Fig. 1. By doing so, both the magnitude and the phase of the antenna weights can be controlled, allowing for more flexibility in the beampattern design. This is because, any complex number with an amplitude no larger than 2 can be uniquely decomposed into two complex numbers with modulus 1 [11], i.e.,

$$ae^{j\omega} = e^{j\phi_1} + e^{j\phi_2}, \quad |a| \le 2, \tag{2}$$

where $\omega = \frac{\phi_1+\phi_2}{2}$ and $a = 2\cos\frac{\phi_1-\phi_2}{2}$. Thus, for any given complex beamformer $\mathbf{w}$, one can first normalize it to have a maximum magnitude no larger than 2, then decompose each element of the given beamformer into two unit-modulus numbers based on (2).

With the DPS, one can apply a null-steering beamformer $\mathbf{w}_n$ which creates nulls at given K directions while formulating a mainbeam towards the desired direction [12], i.e.,

$$\mathbf{w}_n = \mathbf{P}\mathbf{a}(\theta_0), \tag{3}$$

where $\mathbf{P} = \mathbf{I}_N - \mathbf{A}(\mathbf{A}^H\mathbf{A})^{-1}\mathbf{A}^H$ is the orthogonal projection matrix, $\mathbf{I}_N$ is an N by N identity matrix and $\mathbf{A} \in \mathbb{C}^{N\times K}$ contains the steering vectors at the K null directions. By sequentially steering the mainbeam to each target while nulling other targets, one can monitor the vital signals of multiple targets with minimum inter-target interference.

3. DOPPLER FREQUENCY FOR VITAL SIGN MONITORING

Let us consider the same DPS phased array described before which is transmitting a continuous-wave (CW) with center frequency f_c. Typically, when we need to estimate target range and angle, frequency-modulated continuous-wave (FMCW) is used. Here, for simplicity, we focus on resolving targets in the angular domain only, and for that purpose, CW suffices.

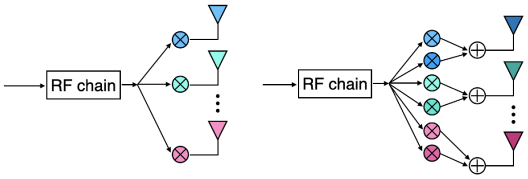

Fig. 1. Left: Phased array. Right: DPS phased array.

The complex envelope of the baseband signal can be written as

$$x(t) = Ae^{j2\pi(f_c t+\phi_0+\Delta\phi(t))}, \tag{4}$$

where A is the amplitude, ϕ_0 is the initial phase of the signal and $\Delta\phi(t)$ is the phase noise of the transmitter.

Assuming that there is a human object at range R_0, the round trip delay of the transmitted signal can be modeled as

$$\tau(t) = \frac{2R_0 + R(t)}{c}, \tag{5}$$

where $R(t)$ is the chest movement due to vital activities. Assuming that the weights of TX are set to formulate a beam towards the human object, the received signal can be expressed as

$$y(t) = \beta Nx(t-\tau(t))e^{j2\pi f_d(t)t} + n(t), \tag{6}$$

where the complex coefficient β accounts for the propagation loss and the target radar cross section (RCS); $f_d(t)$ is the Doppler frequency shift due to the movement of the chest; and $n(t)$ is noise, which is assumed to be white with zero mean and variance σ_n^2.

Since the round trip delay is very small and the phase noise $\Delta\phi(t)$ varies slowly, one can approximate that $\Delta\phi(t) \approx \Delta\phi(t-\tau(t))$, thus after mixing with the conjugate of the transmitted signal $x^*(t)$, we have

$$s(t) = \beta NAe^{-j2\pi(\frac{2R(t)}{c}+\phi_R)}e^{j2\pi f_d(t)t} + n(t)x^*(t) \tag{7}$$

where $\phi_R = \frac{2R_0}{c}$. The phase of $s(t)$ is determined by both $R(t)$ and $f_d(t)$, while the frequency of $s(t)$ is only determined by $f_d(t)$. The Doppler frequency can be expanded as

$$f_d(t) = 2v(t)f_c/c = 2\frac{dR(t)}{dt}f_c/c, \tag{8}$$

where $v(t) = \frac{dR(t)}{dt}$ is the moving speed of the chest due to vital activities. Since the chest movement can be approximated to be sinusoidal, $v(t)$, as the derivative of $R(t)$, is also sinusoidal and has the same frequency as $R(t)$. Provided that the Doppler frequency $f_d(t)$ is linearly proportional to $v(t)$, these two terms have the same frequency. Thus the frequencies of vital signals can be found by estimating the frequency of the signal $f_d(t)$.

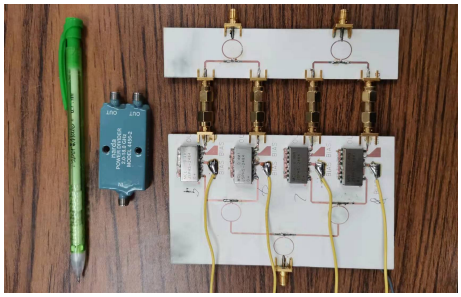

Fig. 2. Left: commercial power divider and a pen. Right: self-fabricated double-phase shifter transmitter.

In order to estimate the frequency of $f_d(t)$, we need to first sample $f_d(t)$ across time, and then apply a Discrete Fourier Transform (DFT) on the samples. To estimate $f_d(t)$ at different times, one needs to first sample $s(t)$ at a frequency much higher than frequency of $f_d(t)$ and segment the time into small segments. In that case, the $f_d(t)$ can be considered constant within each segment, only changing between segments. Then by performing a DFT on the samples of $s(t)$ within a segment, we can estimate the corresponding $f_d(m)$ where $m \in \{1, 2, \ldots, M\}$ is the segment index. After estimating $f_d(m)$ in M segments, the corresponding frequency of $f_d(m)$ can be estimated via a DFT on the estimated $f_d(m)$.

4. IMPLEMENTING DPS PHASED ARRAY

In this section, we describe the implementation of a DPS phased array (see the right side of Fig. 1). We first designed two sets of one-to-four-to-two Wilkinson power divider network and fabricated them on a RO4360 PCB board (see the right side of Fig. 2). In each one-to-four-to-two Wilkinson power divider network, we put four voltage-control phase shifters at each branch in the one-to-four power divider part, thus each phase shifter will have the same input signal. Then the two sets of power divider network are connected via a commercial power divider (see the left side of Fig. 2).

A National Instruments (NI) commercial Signal Defined Radio (SDR) device USRP-2920 is utilized as both the signal source and receiver, which operates over the frequency ranging from 50 MHz to 2.2 GHz and can be easily controlled by the graphical programming software LabVIEW [13].

5. NUMERICAL RESULTS

In this section, the performance of the proposed DPS phased array is validated via experiments and compared with a conventional phased array. In the experiments, by giving a weight vector with unit modulus, the self-fabricated DPS phased array actually worked as a conventional phased array.

The experiment setup is shown in Fig. 3. Two program-controlled actuators loaded with copper boards were used to mimic the movement of human chest (see the right side of Fig. 3). The movement of actuators was set to approximate the human chest movement [14, 15]. The first actuator (target 1) was set to move at 0.6 Hz and another one (target 2) moved

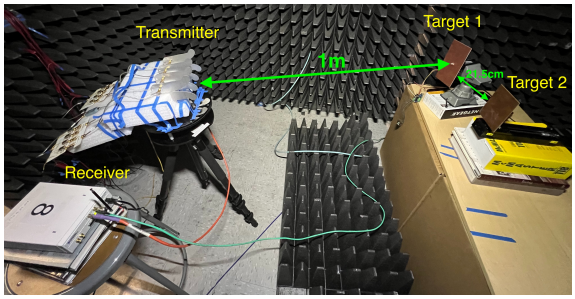

Fig. 3. Experiment setup.

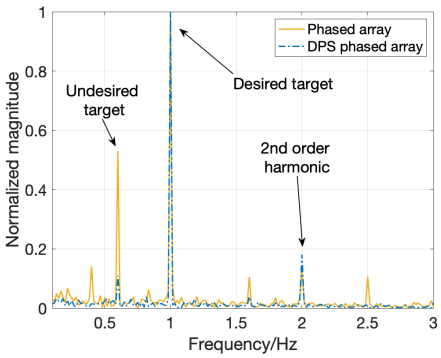

Fig. 4. Comparison between a conventional phased array and a DPS phased array when the desired target is at 5° while moving at 1 Hz.

at 1 Hz. The two actuators were closely placed, with the angle between their centers and the radar equal to 15°. A USRP-2920 equipped with an Omni-antenna was used to generate the baseband signal and receive the echo (see the left side of Fig. 3). The transmitted signal, which was a 10 Hz sine wave carried by a 2.2 GHz RF signal was first generated and passed to the DPS array network, and then transmitted by a four-element Vivaldi antenna array. The transmitter was 1m away from the actuators, and the distance between the two actuators was 21.5cm. The Omni-antenna on the USRP-2920 received the signal reflected by the actuators. The sampling rate of the signal was set as 2×10^5 samples per second.

The collected data were processed with the following frequency estimation protocol. We first utilized a short-time Fourier transform (STFT) with a window length 100 to capture the change in Doppler frequency over time. The windows are not overlapping with each other. Based on the sampling rate, each STFT window was 0.5ms long. Thus, the sampling frequency of $f_d(t)$, the time-varying Doppler frequency, was 2000 Hz, which was sufficient to estimate the low-frequency vital sign (typically $0.2 - 5$ Hz). Then by applying a DFT on the estimated Doppler frequencies from previous STFT operations, we estimated the frequency of $f_d(t)$, which is the same as that of the actuators.

In the first experiment, the target at 5° was the desired target and the target at 20° was the undesired one. A null-steering beamformer was generated and implemented on the proposed DPS phased array. The result is shown in Fig. 4 in a

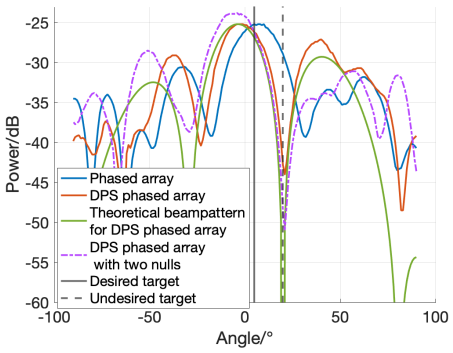

Fig. 5. Measured beampatterns of a conventional phased array and a DPS phased array.

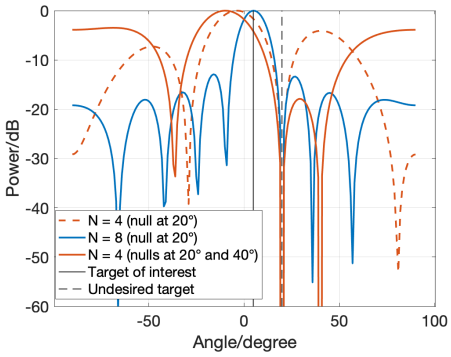

Fig. 6. Theoretical beampatterns of the proposed DPS phased array.

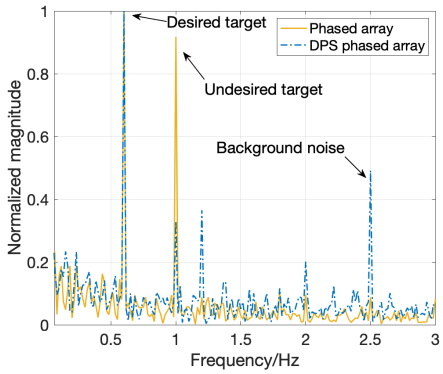

Fig. 7. Comparison between a conventional phased array and a DPS phased array when the desired target is at 20° while moving at 0.6 Hz.

yellow solid line. The frequency estimation result of the corresponding conventional phased array is also plotted in Fig. 4 as the blue dot-dashed line. As one can see, the conventional phased array will detect the frequencies of both desired and undesired targets, while for the proposed DPS phased array, by implementing a null-steering beamformer with a null at 20°, the magnitude of the undesired target drops from 0.53 to 0.11. This 79.25% reduction in the magnitude at 1 Hz indicates sufficient nulling of the undesired target.

To further evaluate the performance, we measured the beampatterns of a conventional phased array and a DPS phased array in an anechoic chamber room using the antenna measurement studio, which are plotted in Fig. 5 in blue and orange lines, respectively. The theoretical beampattern for a DPS phased array with ideal phase shifters which could provide any needed unit-modulus phase value is also plotted in Fig. 5 in green. As one can see, the measured beampattern is close to the theoretical beampattern. The deviation from the theoretical beampattern could be due to the fact that, unlike ideal phase shifters, the real-world phase shifters we used have different initial phases and their magnitudes are not constant over different phase values.

Indeed, the power level at 20° (undesired target) is reduced by 13.9dB after applying a complex null-steering beamformer. However, as the deep null is close to the mainbeam, the power level in the mainbeam direction is also reduced by 1dB. The same phenomenon is also observed in the theoretical beampattern. Both the measured and theoretical DPS phased array have a high sidelobe at 40° which could excite undesired targets. To reduce the sidelobe level, one can use more TX (see blue line in Fig. 6), or set the weights to also create a null at 40° (see orange line in Fig. 6). To validate the effectiveness of creating another null at 40°, we measured the corresponding beampattern and plotted it in Fig. 5 as the purple dot-dashed line; it can be seen that adding another null at 40° reduces the sidelobe level by around 7dB.

In the second experiment, the desired target was the one at 20°. The frequency estimation results are given in Fig. 7, where the yellow solid line refers to the proposed DPS phased array, and the blue dot-dashed line refers to the conventional phased array. Still, the conventional phased array detected both targets, while the proposed DPS phased array creates a null in the direction of the undesired target. In Fig. 7, with the improved beamforming capability from the use of DPS, the DPS phased array reduced the magnitude of the undesired target by 64.13%, from 0.92 to 0.33, which was lower than the second order harmonic of the desired target. From Fig. 4 and Fig. 7 we can see that the proposed DPS phased array with its improved beamforming capability can mitigate the interference from undesired targets, and has the ability to individually monitor the vital signals from multiple closely placed targets with only a modest increase of the hardware cost.

We should note that the cost of a fully digital array with N antennas, and that of a DPS system with M antennas, both operating at 2.2 GHz is, respectively, \$$5491N$ and \$$(66.58M+5491)$ (the cost of a phase shifter is \$33.29 [16], and the cost of a USRP device is \$5491 [17]).

6. CONCLUSION

In this paper, we have designed and fabricated a DPS phased array which is endowed with improved beamforming capability. Through experiments, we have seen that, by applying a complex beamformer, the proposed DPS phased array is capable of mitigating interference from other targets and individually estimating the vital signals of multiple closely placed targets, while slightly increasing the hardware cost.

7. REFERENCES

[1] Fu-Kang Wang, Chung-Tse Michael Wu, Tzyy-Sheng Horng, Chao-Hsiung Tseng, Shiang-Hwua Yu, Chia-Chan Chang, Pin-Hsun Juan, and Yichao Yuan, "Review of self-injection-locked radar systems for noncontact detection of vital signs," *IEEE Journal of Electromagnetics, RF and Microwaves in Medicine and Biology*, vol. 4, no. 4, pp. 294–307, 2020.

[2] Yichao Yuan, Austin Ying-Kuang Chen, and Chung-Tse Michael Wu, "A high-sensitivity low-power vital sign radar sensor based on super-regenerative oscillator architecture," in *2020 IEEE/MTT-S International Microwave Symposium (IMS)*. IEEE, 2020, pp. 651–654.

[3] Ashikur Rahman, Ehsan Yavari, Xiaomeng Gao, Victor Lubecke, and Olga Boric-Lubecke, "Signal processing techniques for vital sign monitoring using mobile short range Doppler radar," in *2015 IEEE Topical Conference on Biomedical Wireless Technologies, Networks, and Sensing Systems (BioWireleSS)*. IEEE, 2015, pp. 1–3.

[4] Changzhan Gu, Guochao Wang, Yiran Li, Takao Inoue, and Changzhi Li, "A hybrid radar-camera sensing system with phase compensation for random body movement cancellation in Doppler vital sign detection," *IEEE Transactions on Microwave Theory and Techniques*, vol. 61, no. 12, pp. 4678–4688, 2013.

[5] T. Hall, B.T. Nukala, C. Stout, N. Brewer, J. Tsay, J. Lopez, R.E. Banister, T. Nguyen, and D.Y.C. Lie, "A phased array non-contact vital signs sensor with automatic beam steering," in *2015 IEEE MTT-S International Microwave Symposium*, 2015, pp. 1–4.

[6] Travis Hall, Donald Lie, Tam Nguyen, Jill Mayeda, Paul Lie, Jerry Lopez, and Ron Banister, "Non-contact sensor for long-term continuous vital signs monitoring: A review on intelligent phased-array Doppler sensor design," *Sensors*, vol. 17, no. 11, pp. 2632, Nov. 2017.

[7] Zhaoyi Xu, Cong Shi, Tianfang Zhang, Shuping Li, Yichao Yuan, Chung-Tse Michael Wu, Yingying Chen, and Athina Petropulu, "Simultaneous monitoring of multiple people's vital sign leveraging a single phased-MIMO radar," *IEEE Journal of Electromagnetics, RF and Microwaves in Medicine and Biology*, pp. 1–10, 2022.

[8] Mehrdad Nosrati, Shahram Shahsavari, Sanghoon Lee, Hua Wang, and Negar Tavassolian, "A concurrent dual-beam phased-array Doppler radar using MIMO beamforming techniques for short-range vital-signs monitoring," *IEEE Transactions on Antennas and Propagation*, vol. 67, no. 4, pp. 2390–2404, 2019.

[9] Nicholas J. Kolias and Michael T. Borkowski, "The development of T/R modules for radar applications," in *2012 IEEE/MTT-S International Microwave Symposium Digest*, 2012, pp. 1–3.

[10] Zhaoyi Xu and Athina P. Petropulu, "Phased array with improved beamforming capability via use of double phase shifters," in *2022 IEEE 12th Sensor Array and Multichannel Signal Processing Workshop (SAM)*, 2022, pp. 66–70.

[11] Xianghao Yu, Jun Zhang, and Khaled B. Letaief, "Doubling phase shifters for efficient hybrid precoder design in millimeter-wave communication systems," *Journal of Communications and Information Networks*, vol. 4, no. 2, pp. 51–67, 2019.

[12] Benjamin Friedlander, "On transmit beamforming for MIMO radar," *IEEE Transactions on Aerospace and Electronic Systems*, vol. 48, no. 4, pp. 3376–3388, 2012.

[13] Rick Bitter, Taqi Mohiuddin, and Matt Nawrocki, *LabVIEW: Advanced programming techniques*, Crc Press, 2006.

[14] Jingtao Liu, Yuchen Li, Changzhi Li, Changzhan Gu, and Jun-Fa Mao, "Accurate measurement of human vital signs with linear FMCW radars under proximity stationary clutters," *IEEE Transactions on Biomedical Circuits and Systems*, vol. 15, no. 6, pp. 1393–1404, 2021.

[15] Yichao Yuan, Austin Ying-Kuang Chen, and Chung-Tse Michael Wu, "Super-regenerative oscillator-based high-sensitivity radar architecture for motion sensing and vital sign detection," *IEEE Transactions on Microwave Theory and Techniques*, vol. 69, no. 3, pp. 1974–1984, 2021.

[16] Mini-circuits, "Phase shifter JSPHS-2484," `https://www.minicircuits.com/WebStore/dashboard.html?model=JSPHS-2484\%2B`.

[17] National Instruments, "USRP-2920," `https://www.ni.com/en-us/support/model.usrp-2920.html`.